

Adipose Stem Cells with Conditioned Media for Treatment of Acne Vulgaris Scar

Xing Shan¹ · Jong Hyeon Choi¹ · Ki Joo Kim¹ · Yoon Jae Lee¹ · Yeon Hee Ryu² · Su Jin Lee¹ · Suk-Ho Moon¹ · Jong Won Rhie^{1,2}

Received: 2 November 2017 / Revised: 27 November 2017 / Accepted: 27 November 2017 / Published online: 16 January 2018
© The Korean Tissue Engineering and Regenerative Medicine Society and Springer Science+Business Media B.V., part of Springer Nature 2018

Abstract This study was to investigate the effect of subcutaneous injection of the adipose stem cells (ASCs) with conditioned media (CM) in the treatment of acne vulgaris scar. We used Adult male New Zealand white rabbit ears as an animal model and induced acne formation by Kignman method. Adipose tissue was isolated and harvested from the scapula of rabbits, and ASCs were cultured and expanded until passage 1. There have four groups in our experiment, include phosphate buffered saline (PBS), ASCs with PBS (ASC + PBS), CM, and ASCs with CM (ASC + CM) group. This solution of 0.6 ml injected to subcutaneous in each group. ASC + PBS and ASC + CM groups were containing ASCs of 5.0×10^6 cells/ml. We analyzed the treatment of 4 groups to scar tissue after 2 and 4 weeks by hematoxylin and eosin stain, immunohistochemistry, and RNA expression level of tumor necrosis factor- α (TNF- α), interleukin-1 α (IL-1 α), and matrix metalloproteinase-2 (MMP-2). Also, the expression of keratin 16 (K16) was detected by western blot analysis. H&E stain showed that infiltration of inflammation cells was significantly reduced at 2 and 4 weeks, as well as re-epithelialization was improved in the ASC + CM group. The ASC + CM group was reduced both expression levels of TNF- α , IL-1 α , and MMP-2 and K16 protein level. In conclusion, the ASCs with CM has a significant curative effect on acne vulgaris scar, more to the point, the CM has a key role on treatment. It could be applied to a therapeutic approach to regenerate to treat acne vulgaris scar.

Keywords Acne vulgaris scar · Adipose stem cell · Acne scar model · Conditioned media · Keratin 16

1 Introduction

Acne scars are divided into atrophic, hyperplastic and keloidal acne scars. Atrophic scars is a common complication of acne vulgaris, are further subdivided into icepick atrophic, boxcar atrophic and rolling atrophic acne scars [1]. Recently, about 20% of the adolescents around the

world are affected by moderate-to-severe acne scars [2], and the probability that this phenomenon continues to occur until the age of 20 years or even 30 years is 64 and 43%, respectively [3]. Specifically, the proportion of Asians in the world who suffer from acne scars is very high due to the fact that their skin is thicker than the Caucasian [4, 5]. In the production of higher quantities of melanin [4, 6] increased number of sebaceous glands, so its led to more sebum secretion. Also, acne scars usually induce a negative psychological impact and social stress on the patient during early scar formation [7].

Kim et al. [8] were the first to report that adipose stem cells (ASCs) were induced wounds healing, scar repair, and fibroblasts activation. In recent years, studies have shown that ASCs exhibit significant therapeutic effect on chronic lesions compared to bone marrow mesenchymal stromal

✉ Jong Won Rhie
rhie@catholic.ac.kr

¹ Department of Plastic and Reconstructive Surgery, College of Medicine, The Catholic University of Korea, 222 Banpo-daero, Seocho-gu, Seoul 06591, Republic of Korea

² Department of Molecular Biomedicine, College of Medicine, The Catholic University of Korea, 222 Banpo-daero, Seocho-gu, Seoul 06591, Republic of Korea

cells (BM-MSCs). There is no significant difference between ACSs and BM-MSCs with respect to surface markers (CD29, CD44, CD90, and CD105), cytokines, and gene expression [9]. However, cell therapy using ASCs is preferred because these cells are easy to isolate and have high relative abundance than BM-MSCs [9]. Moreover, studies suggest that transplanted ASCs accelerate wound healing by expanding the fibroblasts phenotype and increasing the supply of macrophages to the wound, enhancing granulation tissue formation [10–12]. Further studies showed that ASCs promote the growth of dermal fibroblasts through not only intercellular cell-to-cell contact, but also by paracrine activation of marginal cells [13–16]. The ASCs with conditioned media (CM) can stimulate the synthesis of dermal collagen and promote the migration of fibroblasts into the dermis, which are reported to help wrinkle improvement, facial defect filling, and wound healing compared with only ASCs [8]. Few experiments studied show the effects of using the ASCs with CM as an additional treatment when fractional carbon dioxide laser resurfacing (FxCr), so it was shown to cause a significant reduction in erythema and pigmentation [17, 18]. For the treatment of acne scars is also limited to laser therapy and drug therapy. The cell injection therapy has many virtues that wound area is almost zero and it also can effectively prevent further complications, such as erythema and pigmentation caused by laser stimulation. Additionally, it has a direct, short cure time, and also an effective treatment for acne scars compared with a longer course of drug therapy. Thus, we confirmed whether or not ASCs with CM was beneficial effects for wound healing in acne vulgaris scars.

2 Materials and methods

2.1 Preparation of animal model

We used the Kignman method [19] to induce acne formation. Rabbits within the ear of the inner ear tube opening $3\text{ cm} \times 6\text{ cm}^2$ range, smear a thick oleic acid solution of 0.25–0.5 ml once a day for 2 weeks.

2.2 Extract and culture of adipose stem cells

ASCs were extracted from male adult New Zealand white rabbits of scapular region adipose tissue, resected, isolated, and collected in sterile preheated phosphate-buffered saline (PBS; WisentInc., St. Bruno, Quebec, Canada). Finely minced with aseptic scissors, and digested with 0.1% collagenase type I (Sigma, St. Louis, MO) for 30 min at 37 °C in a cellticator (MediKahn, Seoul, Korea). The digested sample was washed twice in Dulbecco's modified Eagle's

medium (DMEM; Gibco, Carlsbad, CA) solution containing 10% fetal bovine serum (FBS; Wisent Inc.) and 1% antibiotic/antimycotic (Gibco), it was then centrifuged three times, at 1300 rpm, for 3 min. The stromal vascular fraction was sifted through a 100- μm strainer (BD Biosciences, San Jose, CA) and was then centrifuged at 1300 rpm for 3 min. The pellets were then resuspended in cell medium; the cells were counted and transferred to a 150 mM dish, placed in 5% CO_2 , incubated at 37 °C for 24 h, washed and removed the non-adherent cells and replaced the culture medium. Subcultures were initiated when the initial cell cultures reached 80–90% confluence. ASCs was sub-cultured to passage 1.

2.3 Subcutaneous injection therapy

Animals in the test were submitted to the same protocol, after established and characterized the formation of the acne scar. All eight male adults New Zealand white rabbit ears were divided into $3 \times 6\text{ cm}^2$ analysis region, and then it was sub-divided into six equal-area treatment regions ($1.5 \times 2\text{ cm}^2$). Experimental group see Table 1 according as ASC + CM, ASC + PBS, CM, and PBS groups that each group is including ASCs of 5.0×10^6 cells/ml with CM, ASCs of 5.0×10^6 cells/ml with PBS, only CM, and only PBS. They were treated on the animal model ears of acne scar. After completed modeling, first injected with each treatment group with 0.6 ml. Then, second injection were administered after 2 weeks (Fig. 1). Intramuscular injection of general anesthesia before treatment, zoletile (Virbac Korea, Korea, 50 mg/ml, 0.3 ml/kg) + xylazine (Bayer Korea, Korea, 23.32 mg/ml, 0.2 ml/kg). Pain management was performed on days 3–7, Daily subcutaneous injections of analgesics ketoprofen (100 mg, 0.06 ml/kg) and antibiotic gentamicin (40 mg/ml, 0.1 ml/kg).

2.4 Histological analysis

Binaural of animals was removed the full-thickness skin on the 2 and 4 weeks. And, it was fixed with a 10% (v/v)

Table 1 Experimental groups and subcutaneous injection volumes

Groups	ASCs density (cells/ml)	Injection volume (ml)
ASC + CM ^a	5.0×10^6	0.6
ASC + PBS ^b	5.0×10^6	0.6
CM ^c	None	0.6
PBS ^d	None	0.6

^aASC + CM: adipose stem cells with conditioned media

^bASC + PBS: adipose stem cells with phosphate buffered saline

^cCM: conditioned media

^dPBS: phosphate buffered saline

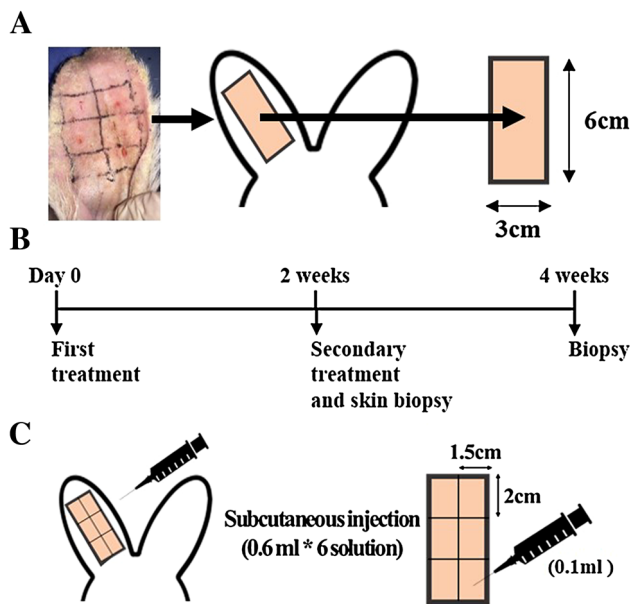


Fig. 1 Experimental design outline. **A** Oleic acid was smeared on the rabbit ears within $6 \times 3 \text{ cm}^2$ for 2 weeks to develop acne formation. **B** First treatment was executed after acne scar formation, and secondary treatment was executed after 2 weeks. Skin biopsy were performed after the rabbits were sacrificed by euthanasia, and the scar area was harvested after 2 and 4 weeks. **C** A subcutaneous injection of $0.1 \text{ ml}/1.5 \times 2 \text{ cm}^2$ of either PBS, ASC + PBS, ASC + CM, or CM were given to each corresponding group, ASC + PBS and ASC + CM groups were containing ASCs of 5.0×10^6 cells/ml

formalin solution, then further embedded in paraffin after tissue dehydration. The sample was further cut into $4 \mu\text{m}$ tissue slices by microtome equipment (rotary type, RM2255, LEICA, Germany), and stained with hematoxylin and eosin. Histological stain observed using a slide scanner (Pannoramic MIDI; 3DHISTECH Ltd., Budapest, Hungary). Measurements of the thickness of epidermis and stratum corneum in $1:200 \mu\text{m}$ scale were performed with Pannoramic Viewer program. Six of one slice on each skin samples were measured and averaged.

2.5 Immunohistochemistry (IHC) staining

Tissue sections were immunostained using COL1A1 (dilution 1:100, Novus Biologicals, USA), COL3A1 (dilution 1:100, Novus Biologicals, USA), anti-MMP-1 mouse monoclonal antibody (dilution $10 \mu\text{g}/\text{ml}$, EMD Millipore, USA). Tissue sections were deparaffinized in xylene, rehydrated through serial dilutions of alcohol, and washed in phosphate-buffered saline. Endogenous peroxidase activity was blocked by incubation with 3% hydrogen peroxide for 10 min at 37°C . Antigen retrieval was performed in a double boiler at microwave 700 W for 30 min and slowly cooling at 37°C for 15 min. Tissues were subsequently incubated with Collagen I alpha 1 antibody,

Collagen III alpha 1 antibody and anti-MMP-1 mouse monoclonal antibody at 37°C in a moist chamber for 12 h. Rabbit IgG antibody (Golden Bridge International Inc, California, USA) was used as a negative control. A Polink-2 DAB kit (Golden Bridge International Inc, California, USA) was used to detect and visualize the bound primary antibodies.

2.6 Real time-quantitative PCR analysis

Total RNA was extracted from the harvested skin tissue using Trizol reagent (Ambion, USA) and genomic DNA was removed using the real-time PCR amplification Kit (Biofact, Seoul, Korea). Synthetic cDNA was obtained by reverse transcription of the RNA, and the expression levels of $\text{TNF-}\alpha$, $\text{IL-1}\alpha$, MMP-2 and GAPDH were detected with SYBR green I master reagent (Roche Diagnostics, Mannheim, Germany) by Light Cycler 480 equipment (Roche, Basel, Switzerland). ΔCt was obtained by measuring the level of GAPDH and the level of gene expression in each group was calculated according to what is described elsewhere [20] and compared with control group. Quantitative analysis was performed using Light Cycler 480 software (Roche, Basel, Switzerland). The primers used for the detection of each gene are listed in Table 2.

2.7 Western blot analysis

Tissue were homogenized to obtain the protein by mechanical (crushing) processes with the further addition of $400\text{--}500 \mu\text{l}$ of T-PER tissue protein extraction reagent (Thermo, IL61101, USA) in an Eppendorf-tube. A proteinase inhibitor cocktail ($4\text{--}5 \mu\text{l}$ from a 100:1 stock, SIGMA, USA) was added to avoid protein degradation and the solution was centrifuged for 15 min at 13,000 rpm at

Table 2 Polymerase chain reaction primer sequences

Gene	Primer	Sequence
$\text{TNF-}\alpha^{\text{a}}$	Reverse	GAAGAGAACCTGGGAGTAGATGAG
	Forward	AGATGGTCACCCTCAGATCAG
$\text{IL-1}\alpha^{\text{b}}$	Reverse	GAGGTGCTGATGTACCAGT
	Forward	CAACAAGTGGTGTCTCCAT
MMP-2 ^c	Reverse	TGAAAGGAGAAGAGCCTGAAGTGT
	Forward	TTGCTGGAGACAAATTCTGGAGAT
GAPDH ^d	Reverse	TCCCGTTCAGCTCGGGGATG
	Forward	TCGGCATTGTGGAGGGGCTC

^a $\text{TNF-}\alpha$: tumor necrosis factor- α

^b $\text{IL-1}\alpha$: interleukin-1 α

^cMMP-2: matrix metalloproteinase-2

^dGAPDH: glyceraldehyde-3-phosphate dehydrogenase

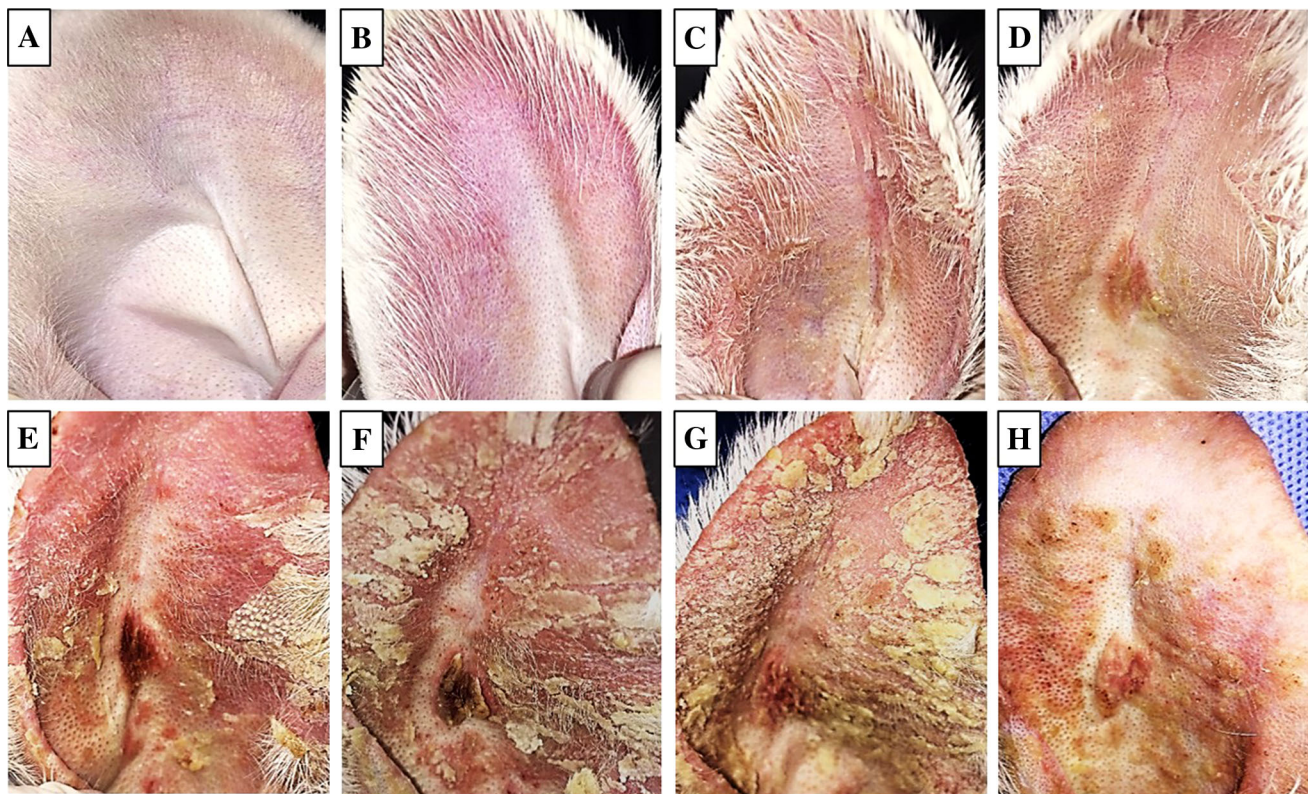


Fig. 2 Acne scar formation upon application of oleic acid on the ear of rabbit and gross changes observed on days **A** 0, **B** 1, **C** 3, **D** 5, **E** 7, **F** 9, **G** 12, and **H** 14

4 °C. The supernatant was collected. The 4 µl of protein solution and 200 µl of quick Start™ Bradford protein assay kit (Bio-Rad, Hercules, CA, USA) solution were added into each well of a 96-well plate for total protein quantification. And, protein concentration was further determined using a softMaxPro software (MDS Analytical Technologies, USA). Protein lysates were added to a SDS sample buffer (ELPIS BIOTECH, Korea) and were further separated by electrophoresis in a 12% sodium dodecyl sulfate polyacrylamide gel (SDS-PAGE), which it was then transferred onto a nitrocellulose blotting membrane (Amersham, Buckinghamshire, UK). Nitrocellulose membrane was revealed after incubation with blocking solution (5% skim milk in Tris-Buffered Saline with 0.1% TWEEN-20 (TBS-T) for 1 h at room temperature (RT), then 3 times washing with TBS-T. Then, the membrane was incubated with primary antibodies of keratin 16 (1:500, Aviva systems biology, California, USA) and β-actin (1:1000, SIGMA, USA) overnight at 4 °C. The membrane was incubated with secondary antibody goat anti-rabbit-HRP (1:5000, Santa cruz biotechnology, Dallas, USA) for keratin 16, or goat anti-mouse-HRP (1:5000, IgG-HRP, Santa cruz biotechnology, Dallas, USA) to β-actin detection respectively for 2 h, after washing 3 times with TBS-T. Immune complexes were analyzed with the addition of the

HRP substrate enhanced chemiluminescence (ECL) detection kit (GE Healthcare Life Sciences, Buckinghamshire, UK), after 3 times washing with TBS-T. And then it was observed using a LAS 4000 (Fujifilm, Tokyo, Japan) and were quantified using the Multi Gauge software (Fujifilm).

2.8 Statistical analysis

Statistical analysis was performed using GraphPad Prism 5.0 software (GraphPad software Inc., La Jolla, CA, USA). Results are shown as mean ± standard deviation. Statistical significance was determined using one-way analysis of variance (ANOVA) with a significance level of *p* value.

3 Results

3.1 Acne scar formation and histological observation

Visual observation revealed that the normal rabbit ear was smooth and pale pink in color, and showed good light transmission, with even capillary distribution (Fig. 2). Also neatly arranged catheter hair follicles, and no acne

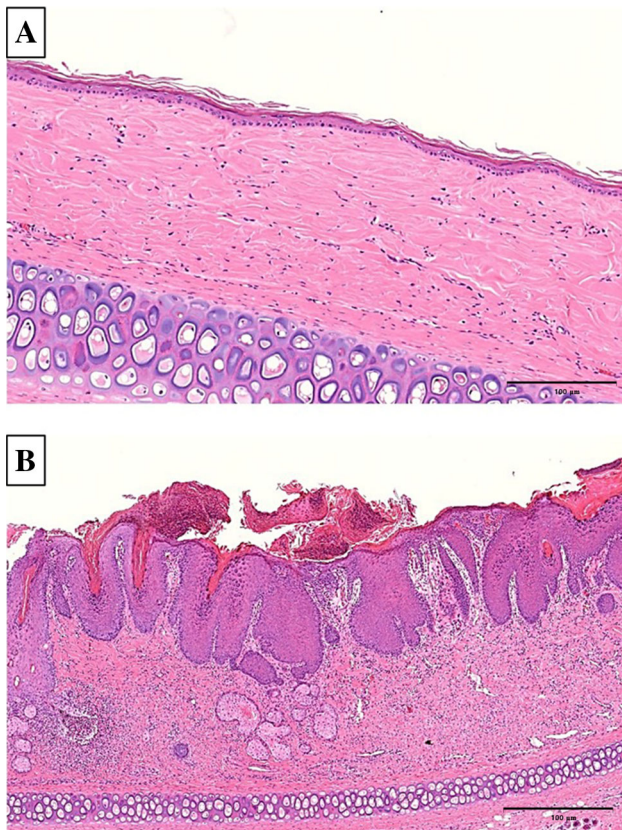


Fig. 3 Hematoxylin-eosin (H&E) staining of sections of **A** the normal control and **B** the acne scar group

(Fig. 2A). The pores began to enlarge, the skin began to keratinize after 3 days (Fig. 2C). And with time, the keratinization aggravated, with gradual uplifting of hair

follicles. All parts of the hair follicle were uplifted and visible white broken rice juice and black bolt on surface. The number of nodes increased significantly. These show that acne scar modeling was completed (Fig. 2H). Significant hyperkeratosis, thickening of the granular layer, stratum spinosum hypertrophy, and hair follicle expansion has been observed in acne scar formation by hematoxylin and eosin (H&E) stain compared with normal control (Fig. 3). Parts of the adjacent hair follicles were integrated with each other, and the hair follicles and funnel were filled with uniform red dye keratosis that extended to the sebaceous glands. Besides, the hair follicle funnel was filled with keratinized material and enlarged pot-shaped. The dermal capillaries were significantly expanded. And, the hair follicles surrounded a large number of inflammatory cells (Fig. 3B). The measurements of the thickness of epidermis and stratum corneum showed that the thickness of epidermis and stratum corneum significantly thickening in acne scar modeling than normal control.

3.2 Visual observation after treatment

After first subcutaneous injection, the horn substitutes and secretions of the sebaceous glands were significantly reduced in the 2 weeks ASC + CM group compared with 2 weeks PBS and ASC + PBS groups (Fig. 4). However, some untreated acnes were still visible in the 2 weeks ASC + CM group. After second injection, visual observation revealed that acne scar in the 4 weeks ASC + CM group were almost cured and hair follicles were narrowed to normal (Fig. 4H).

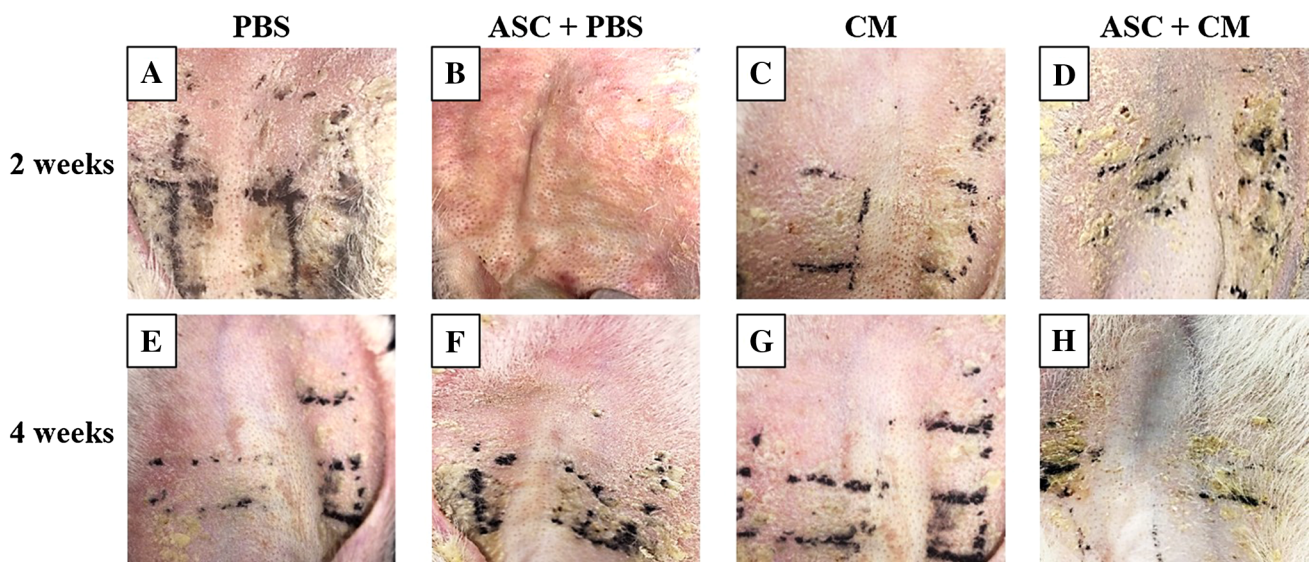


Fig. 4 The observation by naked eyes in phosphate-buffered saline (PBS) group (**A** and **E**), adipose stem cells with PBS (ASC + PBS) group (**B** and **F**), conditioned media (CM) group (**C** and **G**), and

ASC + CM group (**D** and **H**) group. Experimental groups of 2 weeks is **A**, **B**, **C**, and **D**. Experimental groups of 4 weeks is **E**, **F**, **G**, and **H**

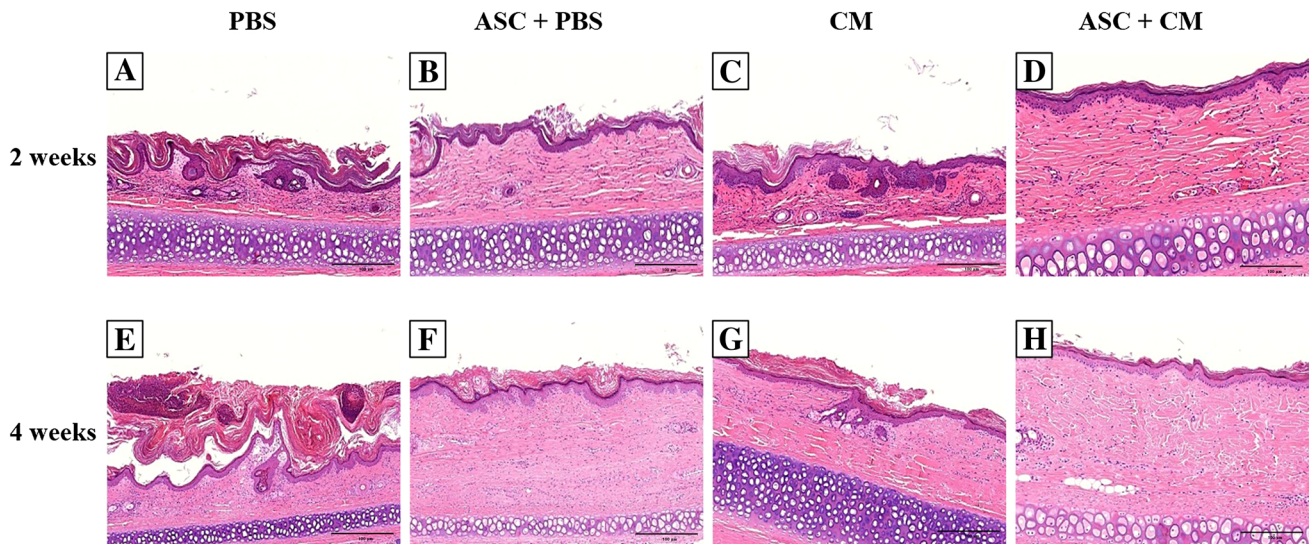


Fig. 5 Histological observation of the effect of treatment in the 2 and 4 weeks groups. H&E stain for histological changes in rabbit ears in the phosphate-buffered saline (PBS) group (A and E), adipose stem

cells + PBS (ASC + PBS) group (B and F), conditioned media (CM) group (C and G), and ASC + CM group (D and H) of 2 and 4 weeks groups

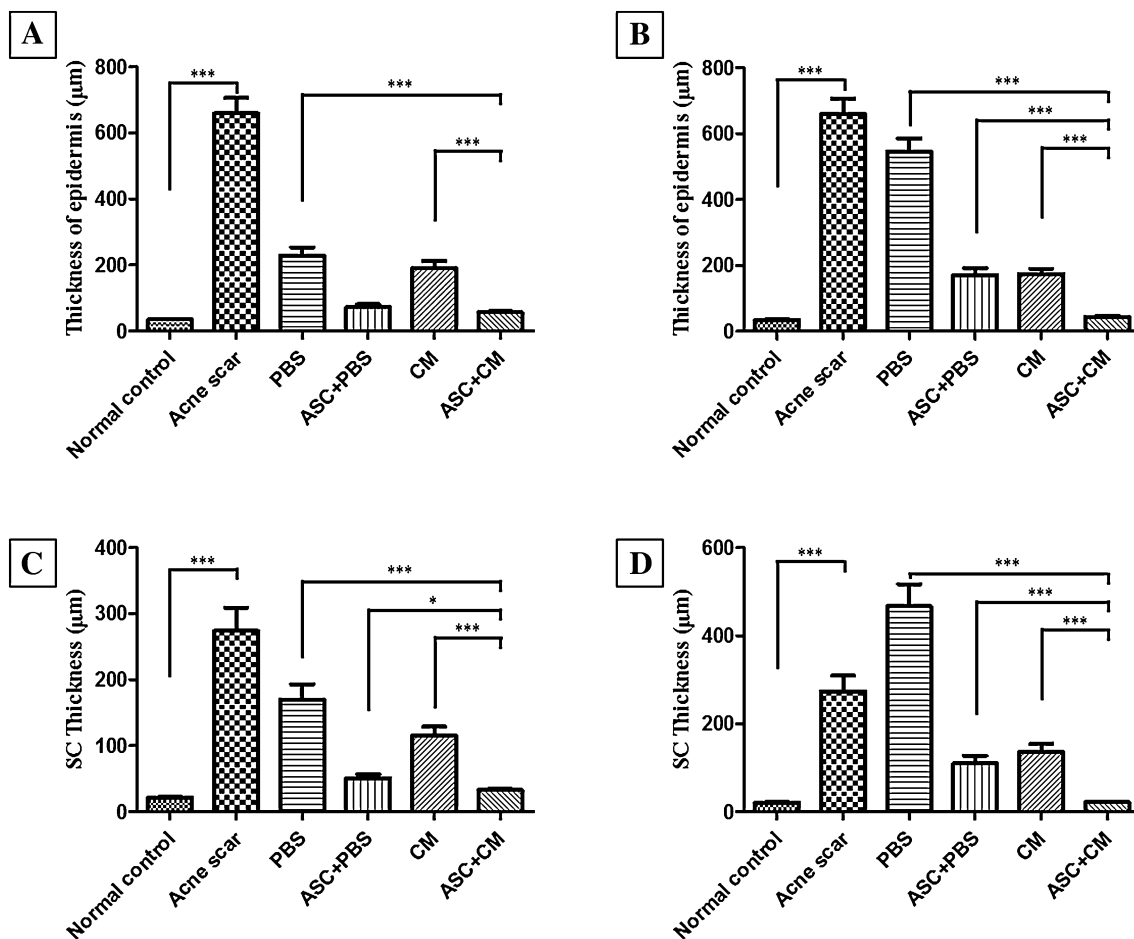


Fig. 6 Thickness of epidermis and stratum corneum in different groups and control groups. A–B Thickness of epidermis in 2 weeks group and 4 weeks group. C–D Thickness of stratum corneum in 2 weeks group and 4 weeks group (** $p < 0.0001$, * $p < 0.01$)

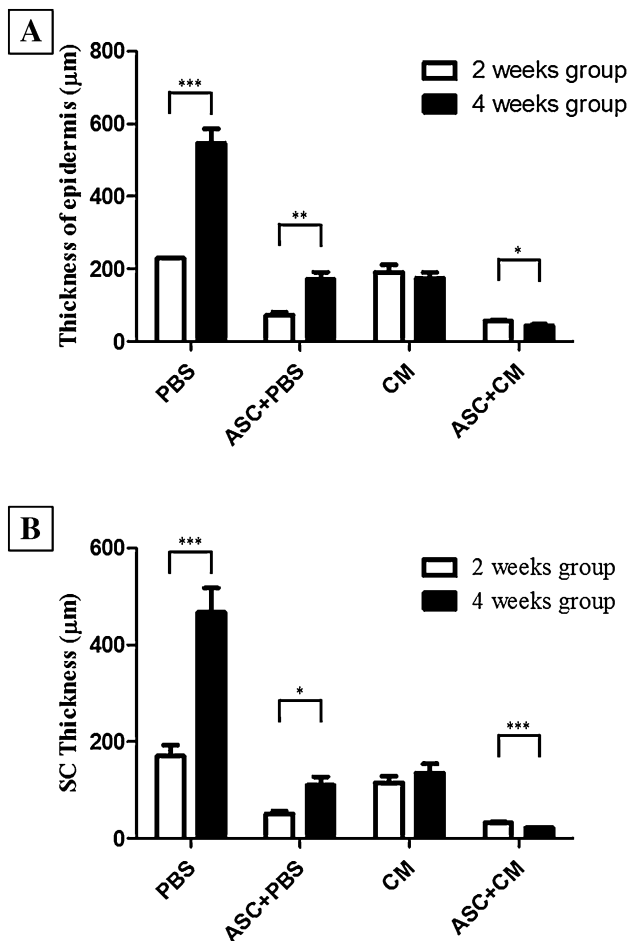


Fig. 7 Thickness of epidermis and stratum corneum in PBS, ASC + PBS, CM, ASC + CM groups. **A** Comparison of epidermal thickness in 2 weeks group and 4 weeks group. **B** Comparison of stratum corneum thickness in 2 weeks group and 4 weeks group (** $p < 0.0001$, ** $p < 0.001$, * $p < 0.01$)

3.3 Histological observation of the effect of treatment

Histological stain showed that the stratum spinosum layers was reduced from the previous hypertrophy to normal 2–3 layers and the number of inflammatory cells was significantly reduced (Fig. 5). Also, Measurements of the thickness of epidermis and stratum corneum showed that significant epidermal thinning in the 2 weeks ASC + CM group comparison to acne scar, PBS, ASC + PBS, and CM group (Fig. 6A, B). However the capillaries were still expanded significantly. The number of stratum spinosum layers was restored to the normal 2–3 layers, and the number of inflammatory cells was significantly reduced in the 4 weeks ASC + CM group. The degree of expansion of the hair follicles was significantly reduced, and the part returned to normal. In addition, the telangiectasia returned to normal (Fig. 5). Measurements of the thickness of

epidermis and stratum corneum showed that significant epidermal thinning in the 4 weeks ASC + CM group comparison to acne scar, PBS, ASC + PBS, and CM group (Fig. 6C). Also, it was similar to normal control group (Fig. 6D). However, loose keratinized substances, inflammatory cell infiltration, and telangiectasia were still visible in the 2 weeks (Fig. 5).

We also found out the thickness of epidermis was significantly increased in PBS and ASC + PBS of 2 weeks group comparison to 4 weeks group. However, it is surprising that the thickness of epidermis was significant thinning in CM and ASC + CM of 4 weeks group comparison to 2 weeks group (Fig. 7A). In addition, the thickness of stratum corneum was significantly increased in PBS, CM and ASC + PBS of 2 weeks group comparison to 4 weeks group, except ASC + CM group (Fig. 7B).

3.4 Immunohistochemical staining of COL1A1, COL3A1, MMP-1

IHC staining of the COL1A1, COL3A1, MMP-1 in normal tissue, acne scar, 2 weeks group and 4 weeks group was performed. This analysis indicated that very strong IHC staining of COL1A1 was observed in acne scar and ASC + PBS of 2 weeks and 4 weeks group, while was not significantly detected in normal tissue, PBS and ASC + CM. We also found the epithelial immunorexpression of MMP-1 and COL3A1 were significantly higher in ASCs-contained groups (ASC + PBS and ASC + CM). And IHC staining of MMP-1 was significantly higher in ASC + CM compared with ASC + PBS in 2 weeks group, but was not detected in PBS group. However, the weaker staining of COL3A1 were observed in ASC + CM of 4 weeks group and similar to normal tissue (Figs. 8, 9, 10). There are very strong IHC staining of COL1A1 and MMP-1 was observed in acne scar (Fig. 8).

3.5 Expression of *TNF-α*, *IL-1α*, and *MMP-2* genes by real-time PCR

TNF-α gene expression was significantly decreased in the 2 weeks ASC + CM group compared with the PBS and ASC + PBS groups (* $p < 0.01$). *IL-1α* gene expression in the 2 weeks ASC + CM group was significantly decreased compared with the PBS group. But, slightly increased compared with the ASC + PBS group (* $p < 0.01$). *MMP-2* gene expression was significantly decreased in the 2 weeks ASC + CM group compared with the acne scar, PBS, and ASC + PBS groups (** $p < 0.001$). The gene expression profiles in the 4 weeks group were similar to those in the 2 weeks group, except for *IL-1α*, which slightly decreased in ASC + CM group compared with the ASC + PBS group (* $p < 0.01$; Fig. 11).

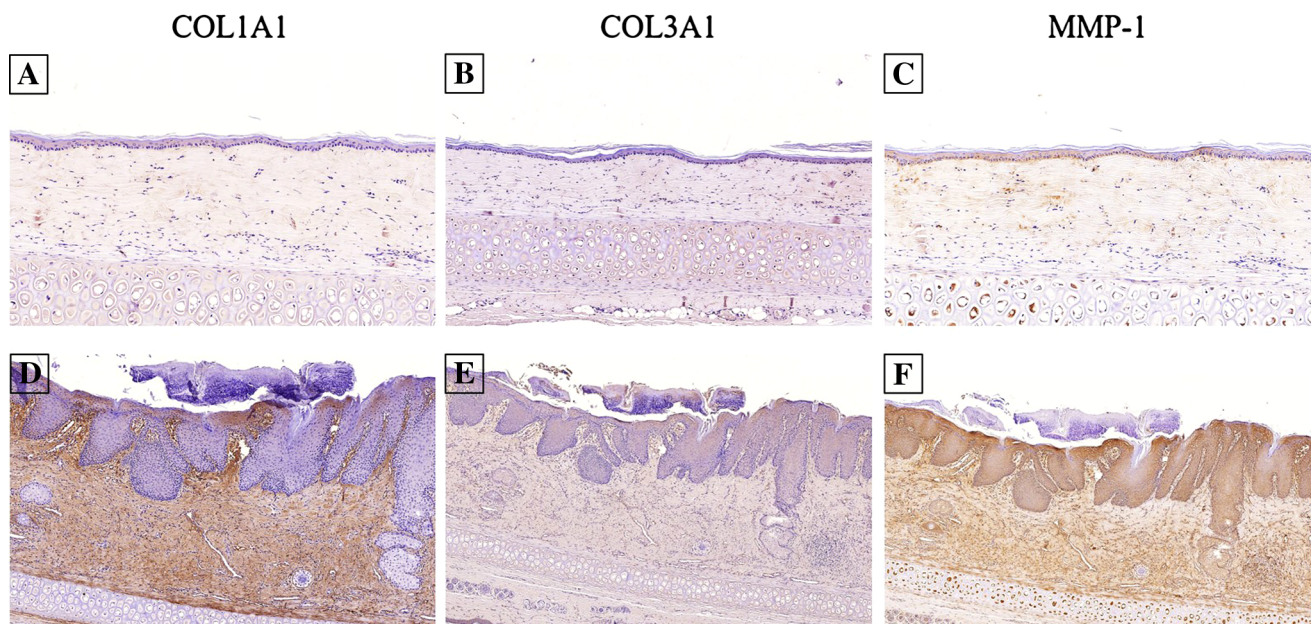


Fig. 8 Immunohistochemistry staining for COL1A1, COL3A1, MMP-1 in normal tissue (A–C) and acne scar (D–F). Scale bar in A–C is 200 μ m, scale bar in D–F is 500 μ m

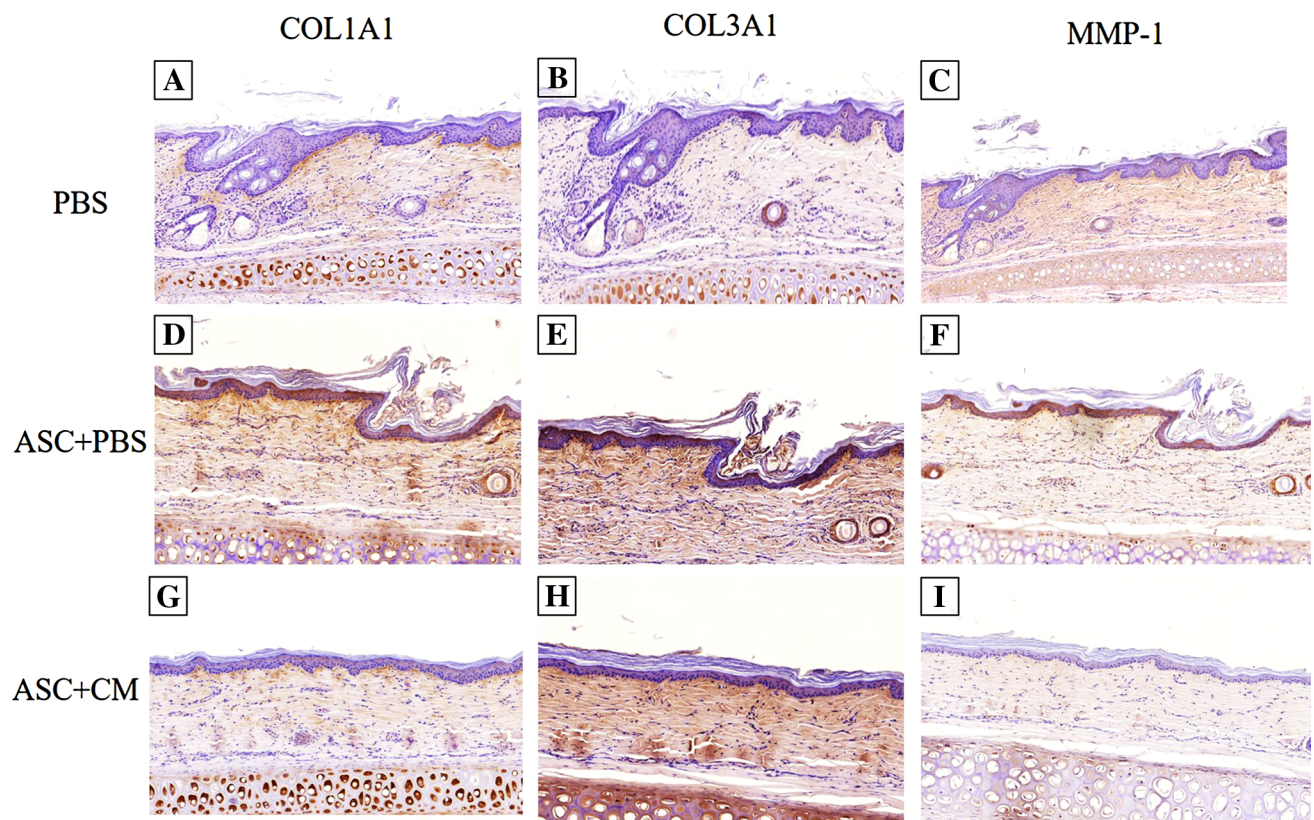


Fig. 9 Immunohistochemistry staining for COL1A1, COL3A1, MMP-1 in PBS (A–C), ASC + PBS (D, E), ASC + CM (G–I) of 2 weeks group. Scale bar in A–I is 200 μ m

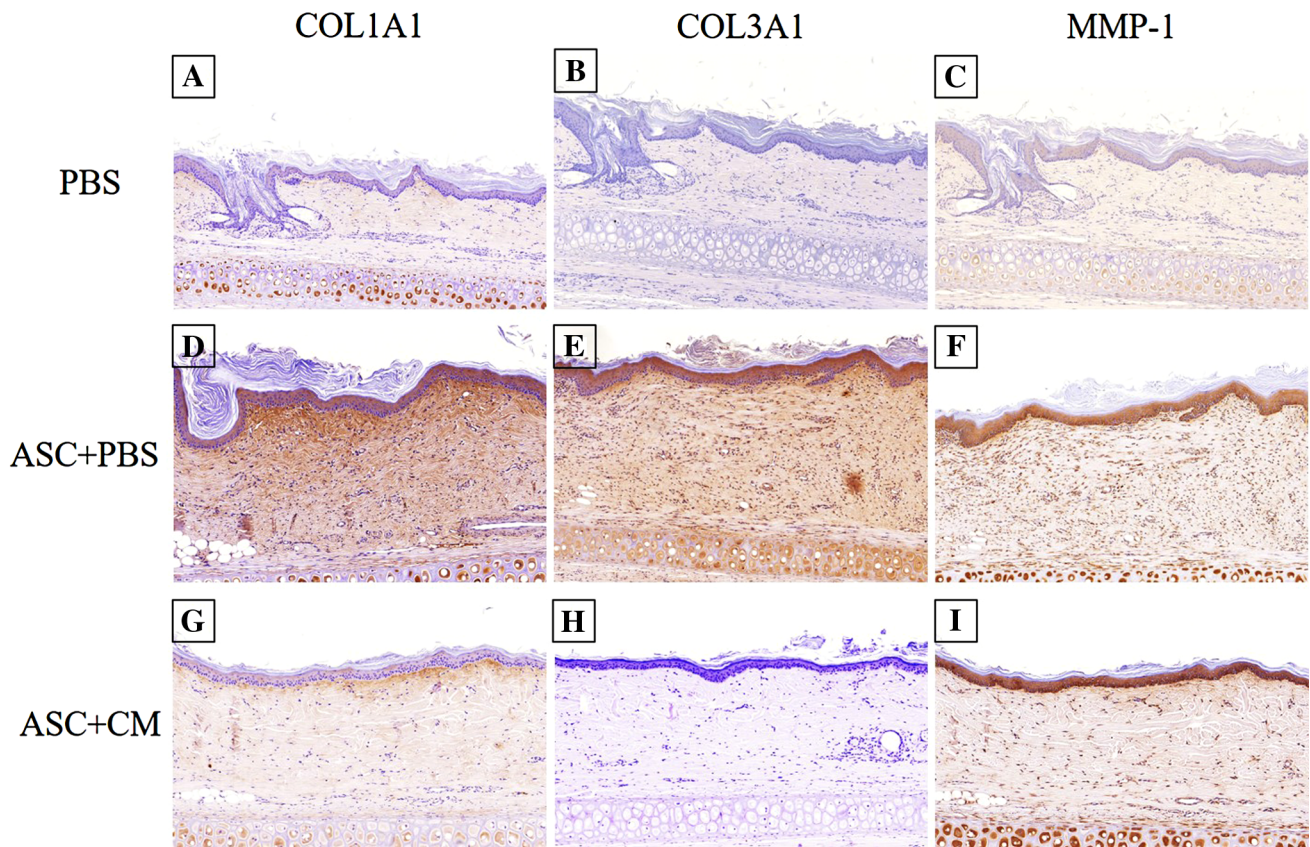


Fig. 10 Immunohistochemistry staining for COL1A1, COL3A1, MMP-1 in PBS (A–C), ASC + PBS (D–E), ASC + CM (G–I) of 4 weeks group. Scale bar in A–I is 200 μ m

3.6 Expression of keratin 16 by western blotting

The keratin 16 protein levels were markedly increased in the acne scar group than in the 2 weeks PBS and ASC + CM groups (** $p < 0.001$). The keratin 16 levels were significantly decreased in the ASC + CM group compared to those in the 2 weeks acne scar and PBS groups (** $p < 0.001$). The keratin 16 levels were decreased in the ASC + CM group compared to those in the 4 weeks acne scar, PBS, and ASC + PBS groups (** $p < 0.001$; Fig. 12).

4 Discussion

Acne is an inflammatory disease of the pilosebaceous duct. It can be caused by abnormal keratinocyte proliferation and desquamation that leads to ductal obstruction, androgen driven increase in sebum production, proliferation of *Propionibacterium acnes*, and inflammation [11, 21, 22]. The treatment of acne has always been one of the hot topics in dermatology, but many experiments are difficult to be done directly on the human. So, there is an urgent need to establish an animal model of acne. Rabbit model is one of

the most commonly acne models which was first used in 1941 and developed in 1989 by the American Dermatology Society. It is one of the more well-studied models of acne [23–25]. In our study, the rabbit ear acne model was successfully established by using the Kligman method.

The pathogenesis of acne is so complicated, but the treatment is still limited to drug therapy and laser therapy. Also, the effect is unsatisfactory. Although some of the drugs on the current market have a good therapeutic effect, but there is still has a big problem. Such as isotretinoin lead to skin desquamation seriously and severe liver toxicity, eye toxicity and teratogenicity. Antibiotic drug resistance [26, 27]. Anti-androgen drugs can lead to hormone levels disorders, also can lead to infertility. Fractional carbon dioxide laser resurfacing(FxCR)is the gold standard for the treatment of atrophic acne scars. However, FxCR is still reported to have a variety of complications, such as post-inflammatory hyperpigmentation, prolonged erythema, skin swelling, infection, and scarring [28–31]. Kim et al. [8] who first confirmed that ASCs were able to heal wounds quickly, repair scarring and activate skin fibroblasts. Also, this study found that ASCs significantly reduced the wound size and accelerated the re-epithelialization from the edge in animal model by secrete several collagens, fibronectin

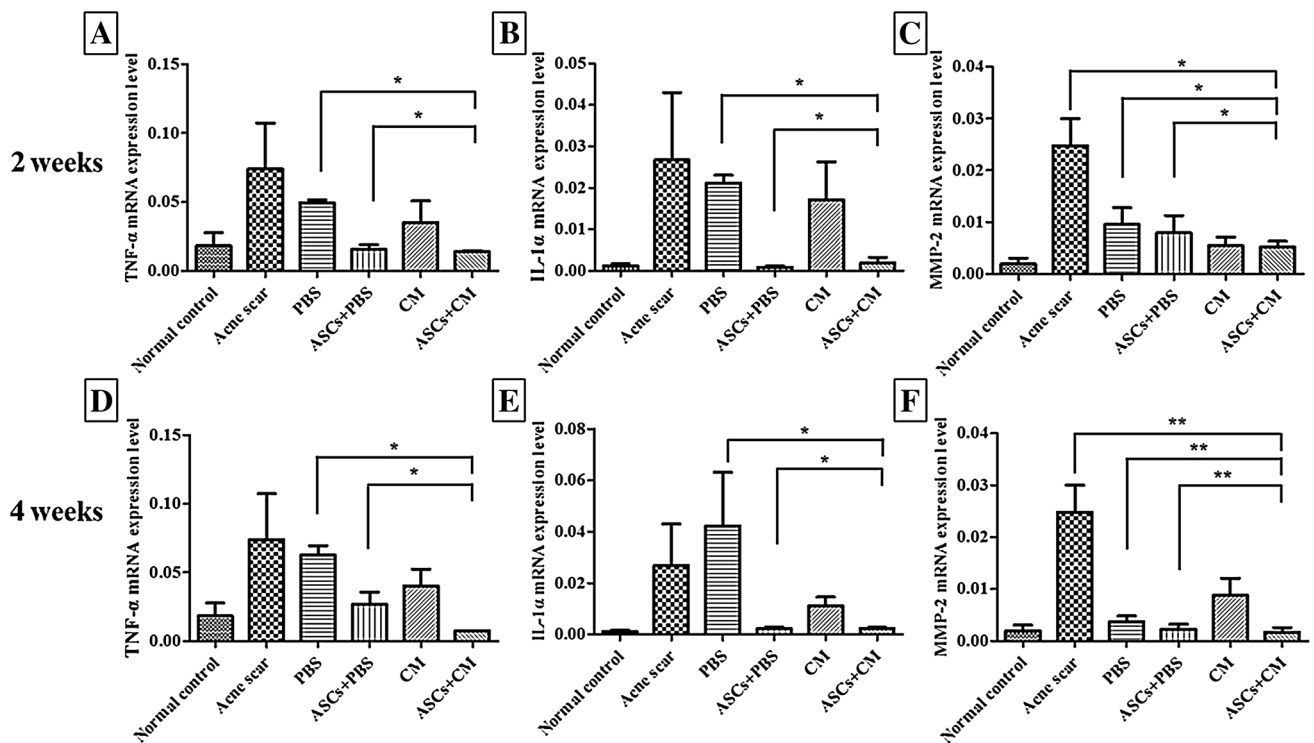


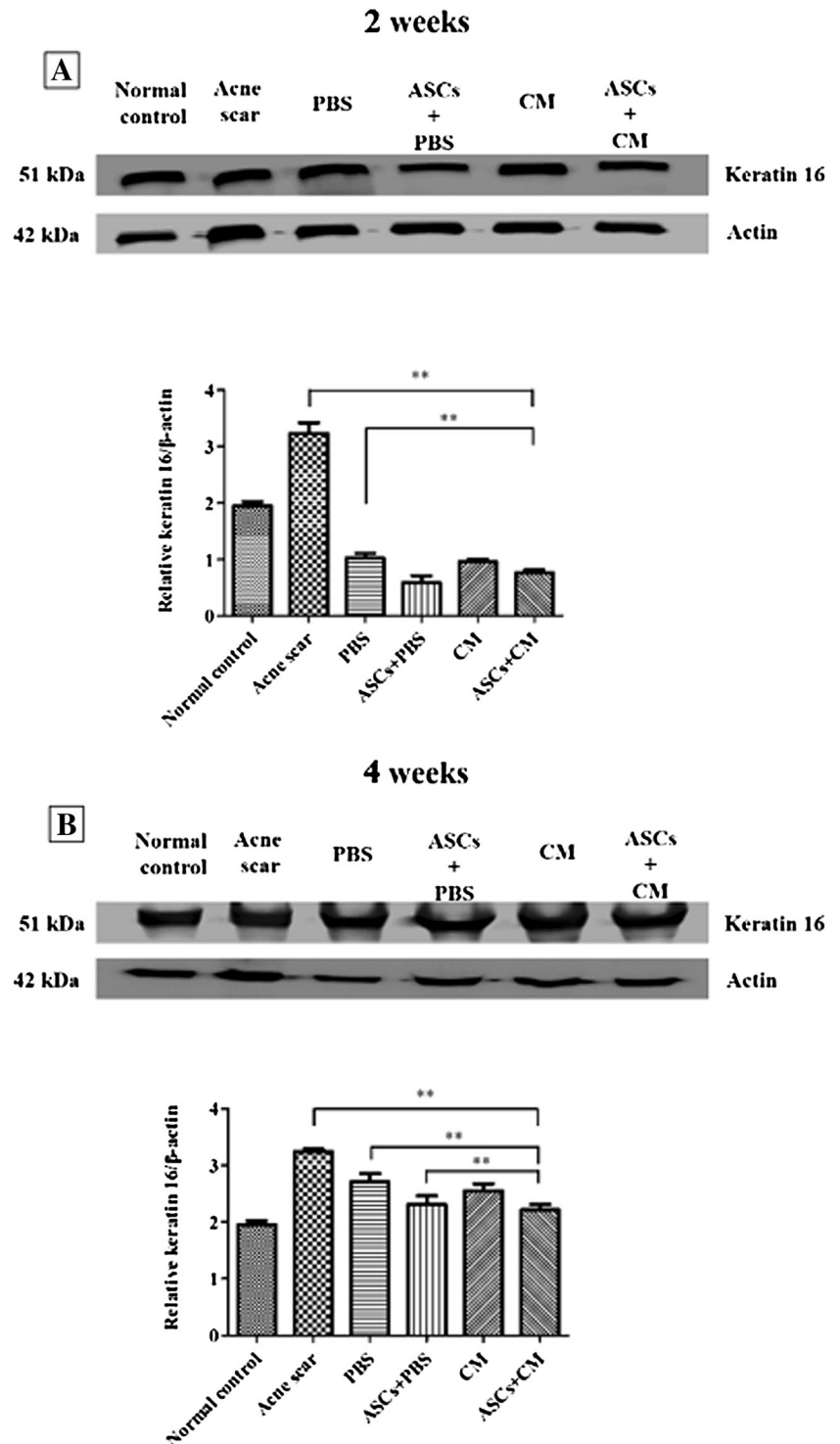
Fig. 11 Real-time quantitative PCR analysis of TNF- α , IL-1 α and MMP-2 gene expression in the 2 and 4 weeks groups. **A** TNF- α , **B** IL-1 α , and **C** MMP-2 gene expression in the 2 week groups. **D** TNF- α ,

E IL-1 α , and **F** MMP-2 gene expression in the 4 weeks groups (* $p < 0.01$, ** $p < 0.001$)

and growth factors. In some studies showed that the expression of MMP-1 in the proliferating keratinocytes may help re-epithelialization [32]. In our study, we found that the epithelial immunoreexpression of MMP-1 in epidermal layer was significantly higher in groups were containing ASCs (ASC + PBS and ASC + CM). We suggested that ASCs significantly accelerated the re-epithelialization. And another studies showed that ASCs promote the growth of dermal fibroblasts by not only through intercellular cell-to-cell contact, but also by paracrine activation of marginal cells [13, 14]. Recently, ASCs were found to accelerate wound healing in human cutaneous wounds [33–35]. Some study have also reported that ASCs is able to produce and secrete a variety of growth factors such as basic fibroblast growth factor (bFGF), keratinocyte growth factor (KGF), transforming growth factor- β 1 (TGF-1 β), hepatocyte growth factor (H-GF), vascular endothelial growth factor (VEGF) and so on [8, 36]. These factors were secreted in conditioned media when ASCs were cultured, so conditioned media (CM) also has a definite influence on wound healing [37]. This study have also found that ASCs with CM can stimulates the synthesis of dermal collagen and migration of the fibroblasts into to the dermis [37]. As an alternative therapeutic strategy for acne scar, we studied the effect of ASCs with CM in acne scar animal model. In our study, pigmentation

and erythema had significant decreased in the 4 weeks ASC + CM group. This decrease in pigmentation is likely because the antioxidant whitening factor in the ASC + CM group which inhibited melanin synthesis and tyrosinase activity in a dose-dependent manner, downregulating the expression of melanogenic proteins (such as tyrosinase-related protein-1 and TGF- β 1) [38, 39]. Scar formation results from fibroblast proliferation, release of cytokines which promote fibrosis, and increased matrix synthesis. Subsequent collagen cross-linking leads to the formation of a mature and stable scar. This process is essential for normal healing [40]. And fibroblasts promote re-epithelialization by the production of ECM proteins such as collagen [41, 42]. In our study we found that fibroblast accumulation at the wound site was increased in acne scar after treatment with ASCs, enhancing COL1A1 and COL3A1 expression, as observed by immunohistochemical staining. However, the higher expression of COL3A1 were observed in ASC + CM compared with ASC + PBS in 2 weeks group. It is indicated that ASC with CM could promote fibroblast migration at the wound site by up-regulation of COL1A1 and COL3A1 genes in the beginning of the wound healing process, compared with normal wound healing and scar treatment by only ASCs [40]. And the staining of COL1A1 was barely detected in ASC + CM of 2 weeks group. This result also suggest that the expression

Fig. 12 Expression of keratin 16 in skin tissue homogenates as assessed by western blotting. β -actin was used as the internal control. **A** Expression of keratin 16 in 2 weeks group. **B** Expression of keratin 16 in 4 weeks group. The protein bands in each gel were quantified using Multi Gauge software. Bar graphs show the relative keratin expression determined as a ratio with respect to β -actin expression



of COL1A1 gene is earlier than COL3A1 in the beginning of the wound healing process.

A previous study showed elevated TNF- α levels in chronic lesions [43]. In addition, IL-1 participates in various physiological and pathological reactions. When the skin is damaged, the epidermal barrier is destroyed and keratinocytes release pre-stored IL-1. Therefore, IL-1

triggers the surrounding keratinocytes to resist damage [44–46]. Many study have shown that Propionibacterium acne can stimulate keratinocytes to produce large amounts of IL-1 α and TNF- α [47–49]. In our study, we found that the TNF- α and IL-1 α levels in the 4 weeks ASC + CM group had decreased by the real-time PCR compared with 2 weeks ASC + CM group.

MMPs are a group of zinc-containing proteolytic enzymes, mainly derived from macrophages that play decisive roles in regulating extracellular matrix synthesis and in processes associated with tissue degradation and remodeling [50, 51]. The levels of TNF- α and other cytokines can be induced with the expression of MMP-2 through the NF- κ B signaling pathway in early stage of acne formation [52, 53]. This affects the production of normal collagen fibers and tissue healing process to promote scar production. In our study, we found that the expression of MMP-2 was increased with the expression of TNF- α . These observations confirmed that MMP-2 expression was related to TNF- α expression in the process of acne inflammation.

Studies have shown that keratin 16 is very active in the process of the epithelial regeneration [54]. In addition, studies have shown that keratin 16 plays a major role in re-epithelialization, which is the first step in repair of skin lesions by mediating accumulation of recombinant keratin filaments in wound edge [55]. The results of western blotting show that the expression of keratin 16 in the 4 weeks group was significantly higher than in the 2 weeks group. This result suggests that the release of keratin 16 was increased during wound healing. And, it is involved that keratin filament recombination in wound edge. The expression level of keratin 16 in the 4 weeks ASC + CM group is the lowest compared with other groups. It is indicated that ASCs with CM accelerate the re-epithelialization.

In summary, this study provides insight into a more direct and effective way by cell therapy to treat acne-like chronic lesions, especially by the adipose stem cell therapy. The cell therapy that is now being used for treatment of major diseases. However, our study is just a small sample pre-clinical study. Further research, a larger sample randomized controlled clinical trial is warranted to verify the results of this study.

Acknowledgements This work was financially supported by a Ministry of Trade Industry and Energy of Korea (10063334 and 10062127) and by National Research Foundation of Korea (NRF) funded by the ministry of Education (2017M3A9E2060428 and 11030383).

Compliance with ethical standards

Conflicts of interest The authors declare that they have no conflict of interest.

Ethical statement We had used adipose tissue excised from rabbit in our experiment. And the experimental protocol was approved by the Department of Laboratory Animal Institutional Animal Care and Use Committee of the Catholic University of Korea (CUMC-2016-0270-03).

References

- Zaleski-Larsen LA, Fabi SG, McGraw T, Taylor M. Acne scar treatment: a multimodality approach tailored to scar type. *Dermatol Surg.* 2016;42:S139–49.
- Kim B, Kim H, Kim JE, Lee SH. Retinyl retinoate, a retinoid derivative improves acne vulgaris in double-blind, vehicle-controlled clinical study. *Tissue Eng Regen Med.* 2013;10:260–5.
- Bhate K, Williams HC. Epidemiology of acne vulgaris. *Br J Dermatol.* 2013;168:474–85.
- McCurdy JA Jr. Considerations in Asian cosmetic surgery. *Facial Plast Surg Clin North Am.* 2007;15:387–97.
- Sykes JM. Management of the aging face in the Asian patient. *Facial Plast Surg Clin North Am.* 2007;15:353–60.
- Shirakabe Y, Suzuki Y, Lam SM. A new paradigm for the aging Asian face. *Aesthetic Plast Surg.* 2003;27:397–402.
- Fife D. Practical evaluation and management of atrophic acne scars: tips for the general dermatologist. *J Clin Aesthet Dermatol.* 2011;4:50–7.
- Kim WS, Park BS, Sung JH, Yang JM, Park SB, Kwak SJ, et al. Wound healing effect of adipose-derived stem cells: a critical role of secretory factors on human dermal fibroblasts. *J Dermatol Sci.* 2007;48:15–24.
- Hong SJ, Jia SX, Xie P, Xu W, Leung KP, Mustoe TA, et al. Topically delivered adipose derived stem cells show an activated-fibroblast phenotype and enhance granulation tissue formation in skin wounds. *PLoS One.* 2013;8:e55640.
- Chen X, Song H, Chen S, Zhang J, Niu G, Liu X. Clinical efficacy of 5-aminolevulinic acid photodynamic therapy in the treatment of moderate to severe facial acne vulgaris. *Exp Ther Med.* 2015;10:1194–8.
- Gollnick H, Cunliffe W, Berson D, Dreno B, Finlay A, Leyden JJ, et al. Management of acne: a report from a Global Alliance to Improve Outcomes in Acne. *J Am Acad Dermatol.* 2003;49:S1–37.
- Ko JY, Lee J, Lee J, Im GI. Intra-articular xenotransplantation of adipose-derived stromal cells to treat osteoarthritis in a goat Model. *Tissue Eng Regen Med.* 2017;14:65–71.
- Xu X, Wang H, Zhang Y, Liu Y, Li Y, Tao K, et al. Adipose-derived stem cells cooperate with fractional carbon dioxide laser in antagonizing photoaging: a potential role of Wnt and β -catenin signaling. *Cell Biosci.* 2014;4:24.
- Kim WS, Park BS, Park SH, Kim HK, Sung JH. Antiwrinkle effect of adipose-derived stem cell: activation of dermal fibroblast by secretory factors. *J Dermatol Sci.* 2009;53:96–102.
- Mehdi E, Michael B. Adult stem cells of orofacial origin: current knowledge and limitation and future trend in regenerative medicine. *Tissue Eng Regen Med.* 2017;14:719–733.
- Park JH, Kim KJ, Rhie JW, Oh IH. Characterization of adipose tissue mesenchymal stromal cell subsets with distinct plastic adherence. *Tissue Eng Regen Med.* 2016;13:39–46.
- Zhou BR, Xu Y, Guo SL, Xu Y, Wang Y, Zhu F, et al. The effect of conditioned media of adipose-derived stem cells on wound healing after ablative fractional carbon dioxide laser resurfacing. *Biomed Res Int.* 2013;2013:519126.
- Azzam OA, Atta AT, Sobhi RM, Mostafa PI. Fractional CO(2) laser treatment vs autologous fat transfer in the treatment of acne scars: a comparative study. *J Drugs Dermatol.* 2013;12:e7–13.
- Fulton JE Jr, Pay SR, Fulton JE 3rd. Comedogenicity of current therapeutic products, cosmetics, and ingredients in the rabbit ear. *J Am Acad Dermatol.* 1984;10:96–105.
- Livak KJ, Schmittgen TD. Analysis of relative gene expression data using real-time quantitative PCR and the 2⁻ $\Delta\Delta$ CT method. *Methods.* 2001;25:402–8.

21. Thiboutot D, Gollnick H, Bettoli V, Dréno B, Kang S, Leyden JJ, et al. New insights into the management of acne: an update from the Global Alliance to Improve Outcomes in Acne group. *J Am Acad Dermatol*. 2009;60:S1–50.
22. Haider A, Shaw JC. Treatment of acne vulgaris. *JAMA*. 2004;292:726–35.
23. Wang J, Liu W, Chen Y, Yan Y. The effect of Shedan mixture in rabbit ear acne model. *Chin J Dermatol*. 2009;9:015.
24. Avci P, Sadasivam M, Gupta A, De Melo WC, Huang YY, Yin R, et al. Animal models of skin disease for drug discovery. *Expert Opin Drug Discov*. 2013;8:331–55.
25. Plewig G, Kligman AM. Rabbit ear model. In: *ACNE and ROSACEA*. London: Springer; 1993. p. 234–9.
26. Reilly BK, Ritsema TS. Managing nonteratogenic adverse reactions to isotretinoin treatment for acne vulgaris. *JAAPA*. 2015;28:34–9.
27. Mills CM, Marks R. Adverse reactions to oral retinoids. An update. *Drug Saf*. 1993;9:280–90.
28. Oh BH, Hwang YJ, Lee YW, Choe YB, Ahn KJ. Skin characteristics after fractional photothermolysis. *Ann Dermatol*. 2011;23:448–54.
29. Metelitsa AI, Alster TS. Fractionated laser skin resurfacing treatment complications: a review. *Dermatol Surg*. 2010;36:299–306.
30. Tierney EP, Hanke CW. Treatment of CO2 laser induced hypopigmentation with ablative fractionated laser resurfacing: case report and review of the literature. *J Drugs Dermatol*. 2010;9:1420–6.
31. Stulhofer Buzina D, Lipozenčić J, Bukvić Mokos Z, Ceović R, Kostović K. Ablative laser resurfacing: is it still the gold standard for facial rejuvenation? *Acta Dermatovenerol Croat*. 2010;18:190–4.
32. Martin P. Wound healing—aiming for perfect skin regeneration. *Science*. 1997;276:75–81.
33. Hassan WU, Greiser U, Wang W. Role of adipose-derived stem cells in wound healing. *Wound Repair Regen*. 2014;22:313–25.
34. Shingyochi Y, Orbay H, Mizuno H. Adipose-derived stem cells for wound repair and regeneration. *Expert Opin Biol Ther*. 2015;15:1285–92.
35. Piłkuła M, Langa P, Kosikowska P, Trzonkowski P. Stem cells and growth factors in wound healing. *Postepy Hig Med Dosw (Online)*. 2015;69:874–85.
36. Koenen P, Spanholtz TA, Maegle M, Stürmer E, Brockamp T, Neugebauer E, et al. Acute and chronic wound fluids inversely influence adipose-derived stem cell function: molecular insights into impaired wound healing. *Int Wound J*. 2015;12:10–6.
37. Zhou BR, Zhang T, Bin Jameel AA, Xu Y, Xu Y, Guo SL, et al. The efficacy of conditioned media of adipose-derived stem cells combined with ablative carbon dioxide fractional resurfacing for atrophic acne scars and skin rejuvenation. *J Cosmet Laser Ther*. 2016;18:138–48.
38. Kim WS, Park SH, Ahn SJ, Kim HK, Park JS, Lee GY, et al. Whitening effect of adipose-derived stem cells: a critical role of TGF- β 1. *Biol Pharm Bull*. 2008;31:606–10.
39. Chang H, Park JH, Min KH, Lee RS, Kim EK. Whitening effects of adipose-derived stem cells: a preliminary in vivo study. *Aesthetic Plast Surg*. 2014;38:230–3.
40. Frantz S, Bauersachs J, Ertl G. Post-infarct remodelling: contribution of wound healing and inflammation. *Cardiovasc Res*. 2009;81:474–81.
41. Al-Mulla F, Leibovich SJ, Francis IM, Bitar MS. Impaired TGF- β signaling and a defect in resolution of inflammation contribute to delayed wound healing in a female rat model of type 2 diabetes. *Mol Biosyst*. 2011;7:3006–20.
42. Crane NJ, Brown TS, Evans KN, Hawksworth JS, Hussey S, Tadaki DK, et al. Monitoring the healing of combat wounds using Raman spectroscopic mapping. *Wound Repair Regen*. 2010;18:409–16.
43. Tarnuzzer RW, Schultz GS. Biochemical analysis of acute and chronic wound environments. *Wound Repair Regen*. 1996;4:321–5.
44. Freedberg IM, Tomic-Canic M, Komine M, Blumenberg M. Keratins and the keratinocyte activation cycle. *J Invest Dermatol*. 2001;116:633–40.
45. Murphy JE, Robert C, Kupper TS. Interleukin-1 and cutaneous inflammation: a crucial link between innate and acquired immunity. *J Invest Dermatol*. 2000;114:602–8.
46. Corsini E, Primavera A, Marinovich M, Galli CL. Selective induction of cell-associated interleukin-1 α in murine keratinocytes by chemical allergens. *Toxicology*. 1998;129:193–200.
47. Huang WC, Tsai TH, Huang CJ, Li YY, Chyuan JH, Chuang LT, et al. Inhibitory effects of wild bitter melon leaf extract on *Propionibacterium acnes*-induced skin inflammation in mice and cytokine production in vitro. *Food Funct*. 2015;6:2550–60.
48. Kim JY, Lee WR, Kim KH, An HJ, Chang YC, Han SM, et al. Effects of bee venom against *Propionibacterium acnes*-induced inflammation in human keratinocytes and monocytes. *Int J Mol Med*. 2015;35:1651–6.
49. Zhang Z, Mu L, Tang J, Duan Z, Wang F, Wei L, et al. A small peptide with therapeutic potential for inflammatory acne vulgaris. *PLoS One*. 2013;8:e72923.
50. Loftus IM, Naylor AR, Goodall S, Crowther M, Jones L, Bell PR, et al. Increased matrix metalloproteinase-9 activity in unstable carotid plaques. *Stroke*. 2000;31:40–7.
51. Wu X, Yang L, Zheng Z, Li Z, Shi J, Li Y, et al. Src promotes cutaneous wound healing by regulating MMP-2 through the ERK pathway. *Int J Mol Med*. 2016;37:639–48.
52. Choi JY, Piao MS, Lee JB, Oh JS, Kim IG, Lee SC. *Propionibacterium acnes* stimulates pro-matrix metalloproteinase-2 expression through tumor necrosis factor- α in human dermal fibroblasts. *J Invest Dermatol*. 2008;128:846–54.
53. Kang S, Cho S, Chung JH, Hammerberg C, Fisher GJ, Voorhees JJ. Inflammation and extracellular matrix degradation mediated by activated transcription factors nuclear factor-kappaB and activator protein-1 in inflammatory acne lesions in vivo. *Am J Pathol*. 2005;166:1691–9.
54. Gawronska-Kozak B, Grabowska A, Kur-Piotrowska A, Kopcewicz M. Foxn1 transcription factor regulates wound healing of skin through promoting epithelial-mesenchymal transition. *PLoS One*. 2016;11:e0150635.
55. Paladini RD, Takahashi K, Bravo NS, Coulombe PA. Onset of reepithelialization after skin injury correlates with a reorganization of keratin filaments in wound edge keratinocytes: defining a potential role for keratin 16. *J Cell Biol*. 1996;132:381–97.